ORIGINAL RESEARCH

Computational Study of Bis-(1-(Benzoyl)-3-Methyl Thiourea) Platinum (II) Complex Derivatives as Anticancer Candidates

Ruswanto Ruswanto[1], Richa Mardianingrum[2], Tita Nofianti[1], Resti Fizriani[1], Siswandono Siswandono[3]

[1]Faculty of Pharmacy, Universitas Bakti Tunas Husada, Tasikmalaya, West Java, Indonesia; [2]Department of Pharmacy, Universitas Perjuangan, Tasikmalaya, West Java, Indonesia; [3]Department of Medicinal Chemistry, Faculty of Pharmacy, Universitas Airlangga, Surabaya, Indonesia

Correspondence: Ruswanto Ruswanto, Email ruswanto@universitas-bth.ac.id

Background: The increasing incidence of cancer every year has resulted in cancer becoming one of the most common causes of death in the world. The most common types of cancer are breast cancer, lung cancer and prostate cancer. Thiourea is one of the compounds that have anticancer effects, and its activity can be increased by structural modifications, one of which involves making a Bis-(1-(benzoyl)-3-methyl thiourea) platinum (II) metal complex.

Purpose: This study aims to obtain platinum (II)-thiourea complex compounds that have a more stable interaction as an anticancer agent compared to cisplatin.

Methods: The methods used are computational studies with molecular docking, simulation of molecular dynamics, and prediction of pharmacokinetics and toxicity.

Results: Based on the molecular docking of the platinum (II)-thiourea complex which has the most stable interaction with lower binding energy than the native ligand and the cisplatin, namely Bis-(3-methyl-1-(naphthalene-2-carbonyl)thiourea)) Platinum (II) against breast cancer receptors (3ERT) and lung cancer (2ITO) and compounds Bis-(1-(3-chlorobenzoyl)-3-methylthiourea) Platinum (II) against prostate cancer receptors (1Z95). The evaluation results of the stability of the interaction using a 50 ns molecular dynamic simulation showed that the Bis-(1-benzoyl-3-methylthiourea) Platinum (II) which binds to the prostate cancer receptor (1Z95) has the most stable interaction. Pharmacokinetic prediction results show that the platinum (II)-thiourea complex has a good pharmacokinetic profile, but there are several compounds that are mutagenic and hepatotoxic.

Conclusion: The Bis-(1-(3,4-dichlorobenzoyl)-3-methyl thiourea) platinum (II) compounds could be a suitable anticancer agent for the lungs.

Keywords: cancer, molecular docking, molecular dynamics, platinum, thiourea

Introduction

Cancer is a large group of diseases that have the same basic properties that are caused by cell division or uncontrolled cell proliferation. This irregular process of division produces a mass of cells in an organ or tissue, which leads to the formation of tumours.[1,2]

Cancer became one of the leading causes of death worldwide in 2018, with a mortality rate of around 9.6 million deaths, and continued to increase until it touched a death rate of 10 million in 2020.[3] The most common types of cancer are breast cancer, lung cancer and prostate cancer.[3]

The increase in the incidence of cancer every year leads to a higher mortality rate. Therefore, it is necessary to develop drugs that can be used for cancer treatment, one of which is drugs that contain metals. A metal widely used for treatment therapy is platinum. The platinum complex has been a mainstay of cancer chemotherapy for more than 25 years.[4] Platinum compounds, especially cisplatin, Solid tumours and hematologic malignancies are managed and treated with the help of the drug cisplatin. It belongs to the class of cytotoxic drugs known as alkylating agents.

Numerous unique platinum complexes have been produced and tested for their anti-cancer capabilities since cisplatin was identified as one of the most effective anti-cancer medications.[4,5] Patients taking platinum medications may also face serious adverse effects, which consequently restricts their use in clinical practice despite their effective results in cancer treatment. In order to reduce the negative effects of these medications, various platinum-based compounds have been created in recent years. According to the findings of this research, Pt (II) complexes have anti-cancer action that is comparable to cisplatin and strongly induces an apoptotic response.[5–9]

One compound that is often used in the treatment of cancer is thiourea.[10,11] In previous studies, several derivatives of 1-benzoyl-3-methyl thiourea have been found to have anticancer activity.[12] In other studies, complexed platinum with thiourea derivatives can increase anticancer activity.[13] So, increasing the anticancer activity of thiourea can be carried out by structural modifications, one of which involves making a platinum (II)-thiourea complex. Based on this, research will be conducted to develop drug candidates in silico by molecular docking and molecular dynamic means, using pharma-cokinetic studies and toxicity predictions to assess compounds from several platinum (II)-thiourea complexes as antic-ancer drug candidates specially for breast cancer, prostate cancer and lung cancer.

Materials and Methods
Materials
The software used includes *AutodockTools*- 1.5.6, *MarvinSketch* version 21.17.0, *Discovery Studio Version* 20.1, *Desmond software for academic license* (D.E. Shaw Research, New York), and web-based programs such as *PDB (Protein Data Bank)* and *pkCSM*. The hardware used is a personal computer with specifications Intel(R) Core(TM) i5-8265U CPU @ 1.60GHz (8 CPUs) x 8.00 GB *of Ram 64-Bit Operating System of Windows 10*. Breast cancer, prostate cancer, and lung cancer receptors were downloaded from the PDB with codes 3ERT, 1Z95, and 2ITO.

Methods
Ligand Preparation
Marvin sketch 5.2.5.1 software was used to draw the ligands, and geometric optimization and protonation were then performed at pH 7.4. Files were saved in the .mrv format. After that, a conformation search was carried out and files were saved in the.pdb and mol2 format.[14] The procedure was carried out for all platinum (II)-thiourea complexes. Ligand preparation was carried out by optimizing the geometry of the formed structure to obtain a stable molecular conformation and low potential energy adapted to the physical condition of the body.[15] The sample thiourea complexes can be seen in Figure 1 and all platinum complexes can be seen in Supplementary Figure S1.
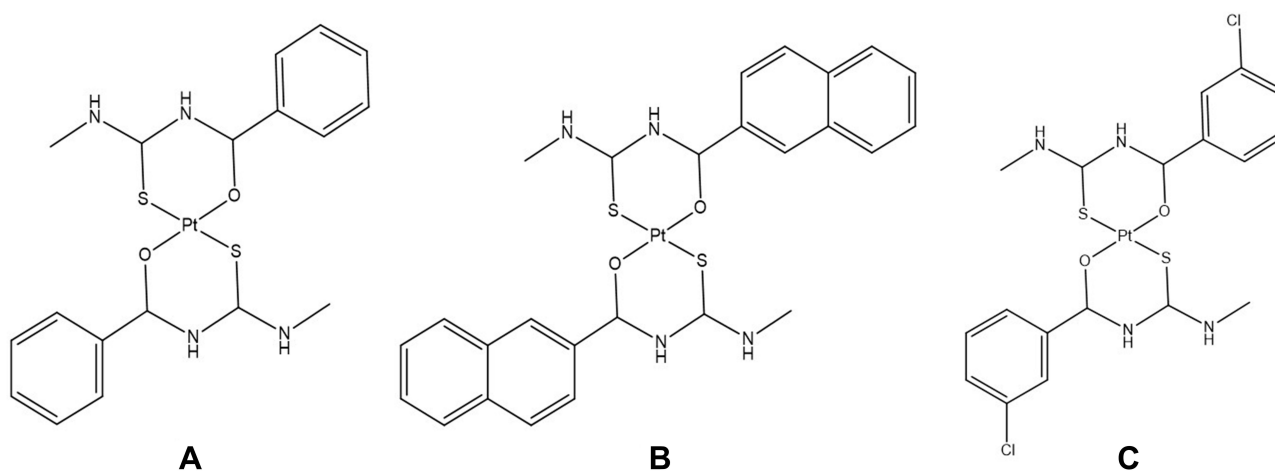

Figure 1 The structure of: (**A**) Bis-(1-benzoyl-3-methylthiourea) platinum (II); (**B**) Bis-(3-methyl-1-(naphthalene-2-carbonyl) thiourea) platinum (II); (**C**) Bis-(1-(3-chlor-obenzoyl)-3-methylthiourea) platinum (II).

Receptor Analysis

Receptor analysis was performed by looking at the Protein Data Bank (PDB) receptor profile on the website http://www.ebi.ac.uk/pdbsum/. After submitting the receptor code, the profile data from the receptor appeared. An ERRAT analysis and 3D VERIFY were then carried out using the site https://saves.mbi.ucla.edu/.

Receptor Preparation, Docking, and Visualisation

Breast cancer, prostate cancer, and lung cancer receptors were downloaded from the PDB with codes 3ERT, 1Z95, and 2ITO, respectively, and were stored in the.pdb format. We then proceeded to the preparation stage, namely the separation of natural ligands, the removal of the solvent molecules and the addition of hydrogen.[16] The addition of hydrogen atoms was also carried out so that the docking atmosphere is close to pH 7. Following optimization, the file was saved in the.pdb format. After that, gasteiger charges were added to the macromolecules using Autodock-Tools software. The addition of the gasteiger charge was designed to adapt to the molecular retaining environment. Non-polar merges were also carried out at this stage, because only polar H atoms are taken into account in the interaction between ligands and receptors. The structures were then saved in the.pdbqt format.

The method to be used must be proven valid through the method validation stage. Validation of the docking method was carried out using the AutodockTools-1.5.6 application by reordering the ligand against its receptors, which had been separated first. The docking method is said to be good if it has a generated Root Mean Square Deviation (RMSD) value ≤ 2Å.[17,18]

The results of molecular docking were analyzed by selecting conformation ligands with the lowest free bond energy (ΔG). The results of docking receptors and ligands were then converted into pdb format and Discovery Studio software was used to analyse the interaction between ligands and active receptor sites.[19]

Molecular Dynamic Simulation

The best candidate structure for the breast cancer, lung cancer and prostate cancer receptor with the platinum (II)-thiourea complex was then determined during molecular dynamics simulation using Desmond software with TIP3P water model and 0.15 M NaCl to mimic physiological ion concentrations.[20] Molecular dynamics simulations were performed at a temperature of 300 K and a pressure of 1.01325 bar in an orthorhombic box with buffer dimensions of 10 Å × 10 Å × 10 Å and an ensemble NPT (Number of atoms, Pressure and Temperature). Energy minimisation was carried out for 100 ps. Each simulation was run for a total of 50 ns with a recording interval of 1.2 ps.[21–23]

Drug Scan

Drug observations were made on all platinum (II)-thiourea complex compounds that had lower free energy than the native ligands. Observations were made using the rules of good medicine (*Lipinski's Rule of Five*), which include lipophilicity < 5, molecular weight < 500 g/mol, hydrogen bond donor < 5, molar refractory between 40–130 and hydrogen bond acceptor < 10. These parameters can be specified using the website http://www.scfbio-iitd.res.in/software/drugdesign/lipinski.jsp.[14]

Drug Scan

Pharmacokinetic properties (absorption, distribution, metabolism and excretion (ADME)) and the toxicity predictions of platinum (II)-thiourea complexes were performed using pkCSM online tools.[24] The complex structure of platinum (II)-thiourea was translated into the SMILES format and the pkCSM online tools (http://biosig.unimelb.edu.au/pkcsm/prediction used to process compounds to predict ADME and compound toxicity.

Results
Receptor Analysis

Receptor analysis was performed on the alpha oestrogen receptor with pdb code 3ERT for breast cancer, the EGFR receptor with the pdb code 2ITO for lung cancer, and the androgen receptor with pdb code 1Z95 for prostate cancer. The crystal structure of each receptor was downloaded from the PDB and saved in a.pdb file format. Images of the structure of each receptor are shown in Figure 2.

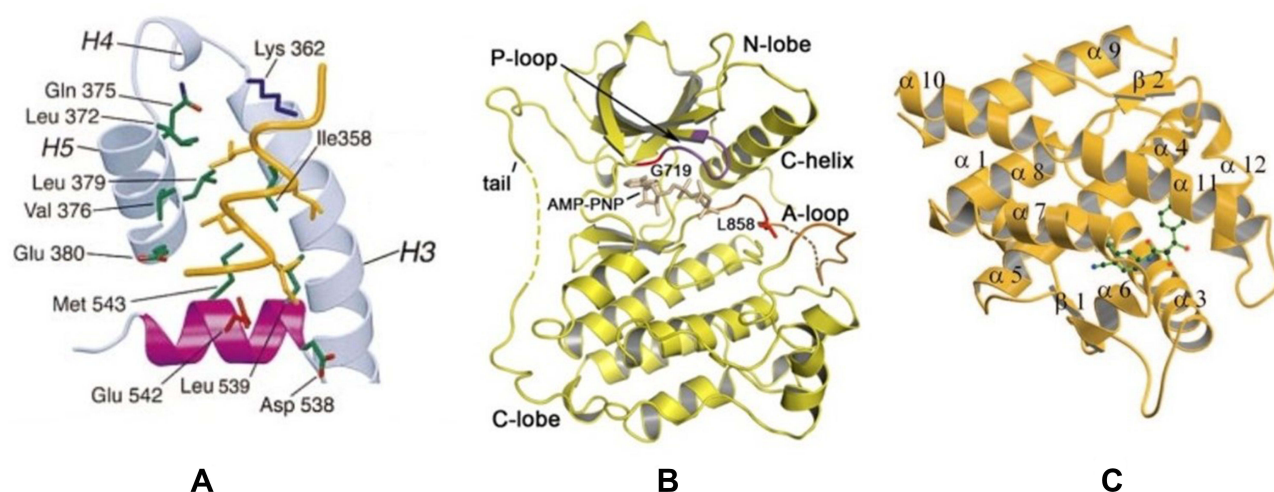**Figure 2** Receptor structure of 3ERT[41] (**A**); 2ITO[42] (**B**); 1Z95[43] (**C**).

The examination of PROCHECK using the Ramachandran plot (Figure 3) focuses on that which has an atypical geometry and allows for the assessment of the structure as a whole. To see if the protein structure has good analysis, results on the Ramachandran plot can be observed using a non-glycine residue plot, where the *disallowed regions* should be less than 0.8%.[25,26]

Based on the Ramachandran plot analysis, the oestrogen receptor alpha (3ERT) had an amino acid residue count in the *most favoured regions* of 91.2%, with the number of amino acid residues in the *disallowed regions* being 0.0%. The EGFR receptor (2ITO) has a 79.8% amino acid residue count in the *most favoured regions*, with an amino acid residue count of 0.4% in the *disallowed regions*. The androgen receptor (1Z95) has 94.4% of amino acid residues in the *most favoured regions*, with 0.0% amino acid residues in the *disallowed regions*. From these results, it was found that the alpha oestrogen receptor (3ERT), EGFR receptor (2ITO) and androgen receptor (1Z95) have a stable protein structure.

ERRAT is a tool used to calculate the consistency of the resulting model by calculating the statistics of certain types of atoms against other atoms and is an approach to finding the wrong fold area in the protein structure. The ERRAT analysis results can be seen in Figure 4.

The following factor quality values were obtained from the results of the ERRAT calculation: 98.319% for the alpha oestrogen receptor (3ERT), 94.096% for the EGFR receptor (2ITO) and 100.00% for the androgen receptor (1Z95). These results show that the protein structures of the oestrogen receptor alpha (3ERT), EGFR receptor (2ITO) and androgen receptor (1Z95) protein structure are of high quality and high resolution, with negligible error criteria for amino acid residues in the modelled fusion protein.[26]

3D VERIFY technology determines the structure of a protein through its three-dimensional visibility. A protein structure is said to be good if it has about 80% with an average score of 3D to 1D ≥0.2.[27] Results of the 3D VERIFY examination for alpha oestrogen receptors, EGFR receptors and androgen receptors can be seen in Figure 5.

The alpha oestrogen receptor (3ERT), EGFR receptor (2ITO) and androgen receptor (1Z95) have 3D VERIFICATION torture results of 80%, 84.16% and 88.66%, respectively, of amino acids that have an average score of 3D to 1D ≥0.2, so they are said to have a good quality structure. From the results of the overall receptor analysis, it can be concluded that the alpha oestrogen receptor (3ERT), EGFR receptor (2ITO) and androgen receptor (1Z95) can be used to perform further computational analyses, including molecular docking and molecular dynamics.

Receptor Preparation, Docking and Visualisation

The initial steps in the preparation of the receptor include the separation of the chain of macromolecules that bind to the target. The receptors of alpha oestrogen, EGFR and androgen identified as 3ERT, 2ITO and 1Z95, respectively, were downloaded from the PDB, and the macromolecular structure of the protein was found to bind to ligands and solvents.

The next step after the separation of the macromolecular chain is the optimisation of the macromolecular structure. The optimisation steps involved the removal of water molecules and the addition of hydrogen atoms. The removal of
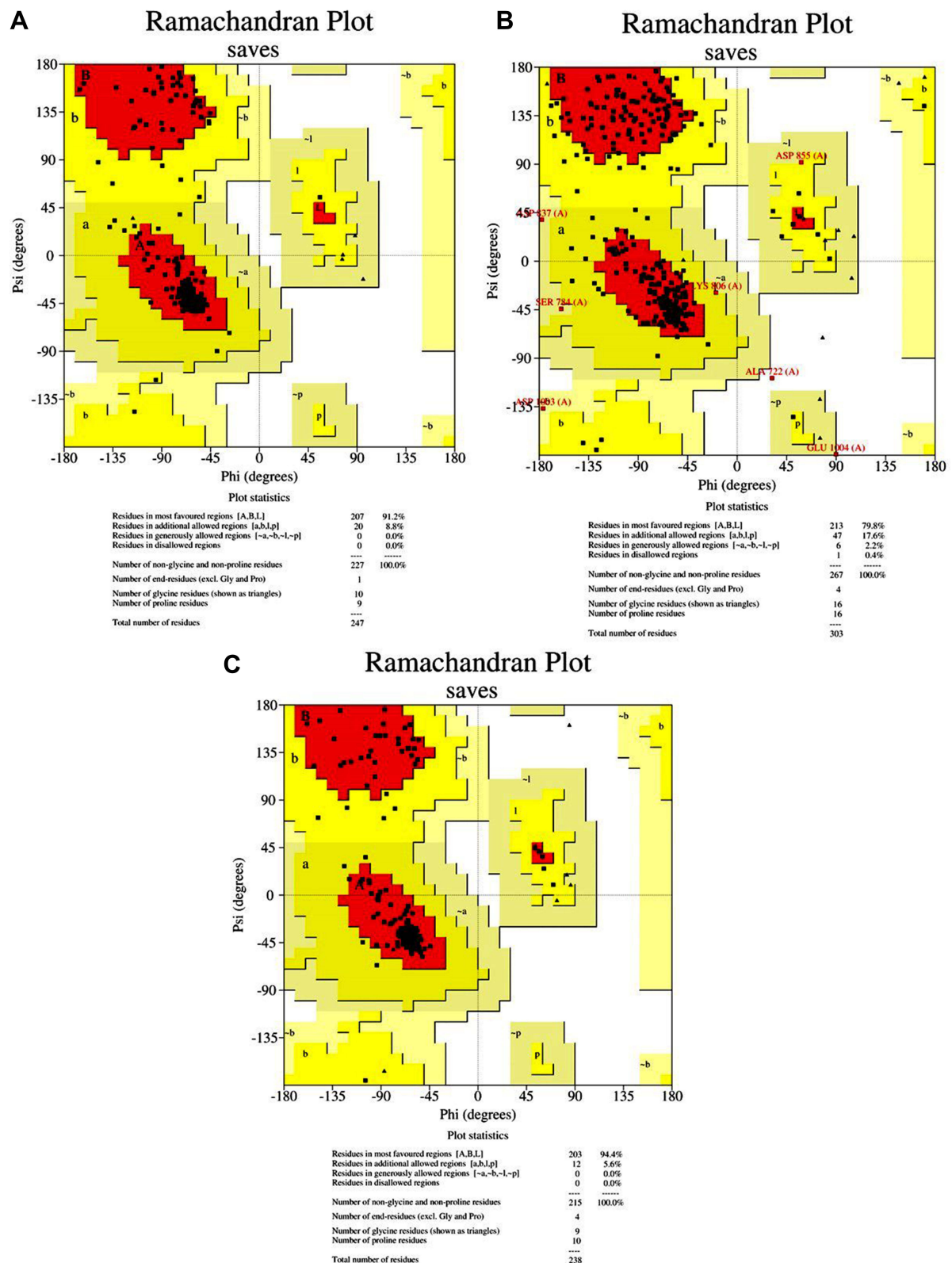
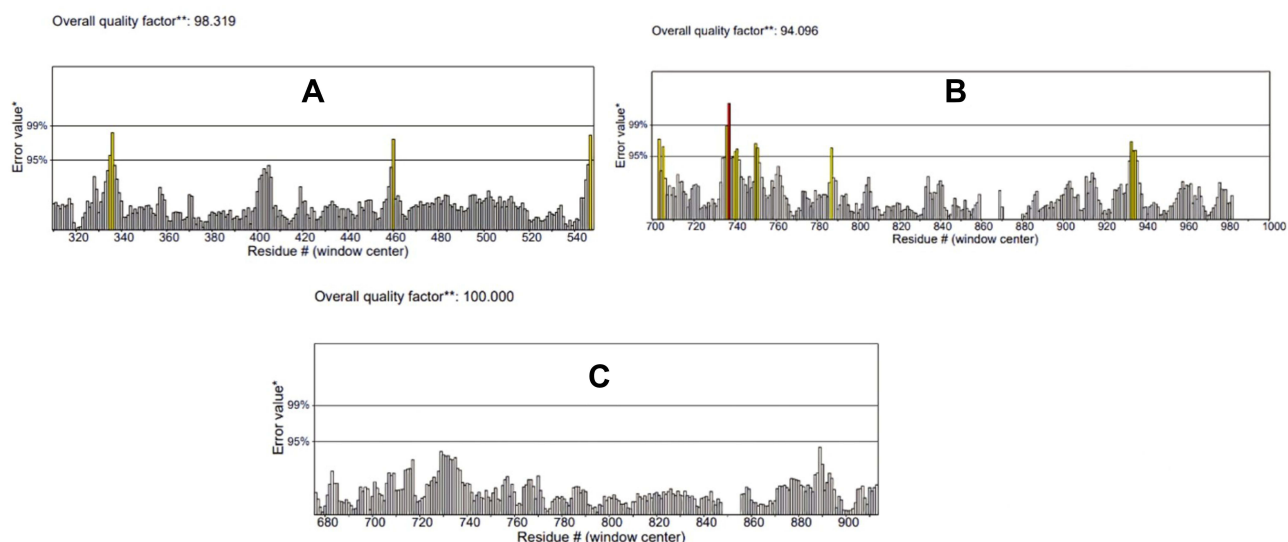Figure 3 Ramachandran plot of 3ERT (**A**); 2ITO (**B**); 1Z95 (**C**).

Figure 4 The ERRAT analysis results of 3ERT (**A**); 2ITO (**B**); 1Z95 (**C**).

water molecules was designed to prevent water from interacting with compounds to be tethered to the receptors.[28] The addition of hydrogen atoms was carried out to re-display hydrogen atoms that are likely to be lost due to the possibility of amino acid structures being damaged at the time of crystallisation by x-ray radiation.[29,30] The addition of hydrogen atoms was also carried out so that the docking atmosphere is close to pH 7.[31] Following optimization, the file was saved in the.pdb format.

After that, gasteiger charges were added to the macromolecules using Autodock-Tools software. The addition of the gasteiger charge was designed to adapt to the molecular retaining environment.[32] Non-polar merges were also carried out at this stage, because only polar H atoms are taken into account in the interaction between ligands and receptors. The structures were then saved in the.pdbqt format.

Validation was carried out using AutodockTools-1.5.6 software. The RMSD is a parameter for evaluating similarities between two structures, based on the differences in the distances of similar atoms.[25] Validation was carried out by the redocking method on the active side of the co-crystalline ligand, namely 4-hydroxytamoxifen for the alpha oestrogen receptor (3ERT), gefitinib for the EGFR receptor (2ITO) and R-Bicalutamide for the androgen receptor (1Z95) on crystallography results (Table 1). The method is said to be valid if the RMSD value $\leq$ 2Å.[17]

The validation results on each receptor show that each receptor has an RMSD value of $\leq$2.0, so the docking method can be said to be valid (Figure 6).

Docking Ligands Against Target Receptors

The results of molecular tethering showed that all platinum (II)-thiourea complex compounds intersected with breast cancer (3ERT), lung cancer (2ITO) and prostate cancer (1Z95) receptors. The three compounds having the lowest binding energy can be seen in Table 2. The detailed docking results can be seen in Supplementary Table S1–S3.

Visualisation of Docking Results

Visualisation of docking results was carried out using Discovery Studio software in 2D and 3D (Figure 7) to see the bonds that occur between ligands with the lowest binding energy and amino acid residues from breast cancer (3ERT), lung cancer (2ITO) and prostate cancer (1Z95) receptors. The types of interactions that occur can be seen in Table 3.

Looking at the interaction between breast cancer receptors (3ERT) and natural ligands, the comparative compound (cisplatin) and platinum (II)-thiourea complex test ligands, an interaction was seen between 4-hydroxytamoxifen (natural ligand) and amino acid residues of 22 bonds, with a total of 3 hydrogen bonds (ARG A:394;
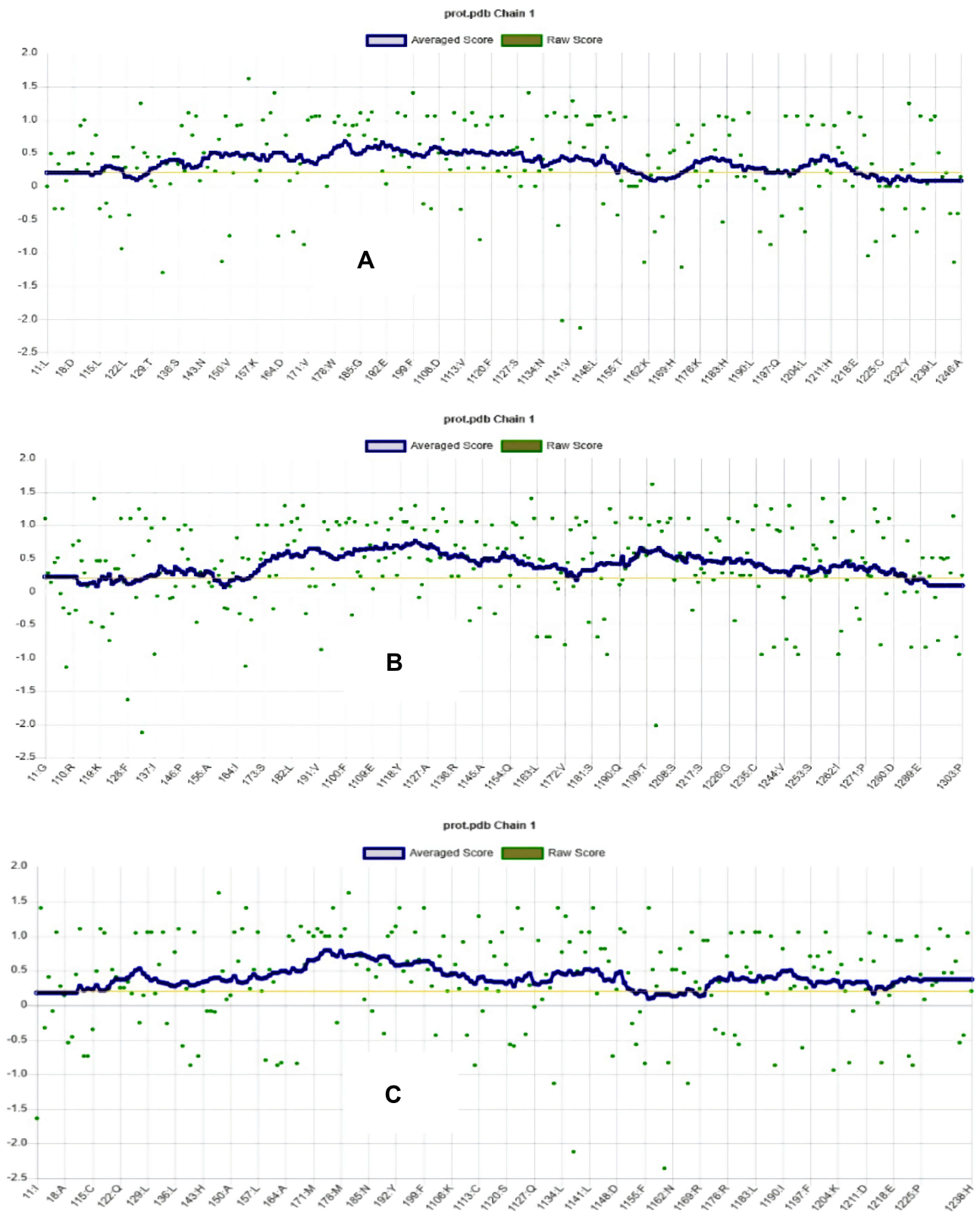
Figure 5 The 3D VERIFY analysis results of 3ERT (**A**); 2ITO (**B**); IZ95 (**C**).

Table I Docking Method Validation Results

PDB Code	Grid Box (Å)			RMSD (Å) ± SD
	X	**Y**	**Z**	
3ERT	30.162	−1.913	24.207	0.81 ± 0.078
2ITO	−48.508	−0.753	−21.855	1.78 ± 0.179
1Z95	27.744	3.191	8.152	1.23 ± 0.021

GLU A:353; THR A:347). There was an interaction between the comparison compound and the amino acid residue of 4 bonds, with as many as 2 hydrogen bonds (THR A: 347; ASP A:351), whereas the platinum (II)-thiourea complex test ligand interacted with as many as 20 amino acid residues, with 2 hydrogen bonds (THR A:347; ASP A:351).

Hydrogen bonds themselves are bonds between positively charged H atoms and other negatively charged atoms, such as N, O and F. In addition to the presence of hydrogen bonds in the interaction between amino acid residues and test ligands, there are hydrophobic bonds, which include pi-sigma, pi-alkyl, van der walls and others. Hydrophobic bonds also play a role in determining the stability of ligands against receptors. Hydrophobic bonds are non-covalent bonds that avoid the liquid environment, minimise the interaction of non-polar residues with water, and tend to form groups next to the globular structure of proteins.[33]

Looking at the interaction between the lung cancer receptor (2ITO) and natural ligands, the comparison compound (cisplatin) and the platinum (II)-thiourea complex test ligand, an interaction was seen between gefitinib (natural ligand) and amino acid residues of 19 bonds, with a total of 1 hydrogen bond (MET A:791). There was an interaction between the comparison compound and the amino acid residue of 6 bonds, with 2 hydrogen bonds (ASP A:855; ASP A:842), whereas the platinum (II)-thiourea complex test ligands interacted with as many as 13 amino acid residues, with 3 hydrogen bonds (ASN A:842; ASP A:800; ASP A:855).

Looking at the interaction between prostate cancer receptors (1Z95) and natural ligands, the comparative compound (cisplatin) and platinum (II)-thiourea complex test ligands, an interaction was seen between R-Bicalutamide (natural ligand) and amino acid residues of 24 bonds, with 2 hydrogen bonds (ARG A:752; THR A:877). There was an interaction between the comparison compound and the amino acid residue of 9 bonds, with as many as 2 hydrogen bonds (GLY A:738; HIS A:874), whereas the platinum (II)-thiourea complex test ligands interacted with as many as 24 amino acid residues, with 1 hydrogen bond (ASN A: 705).
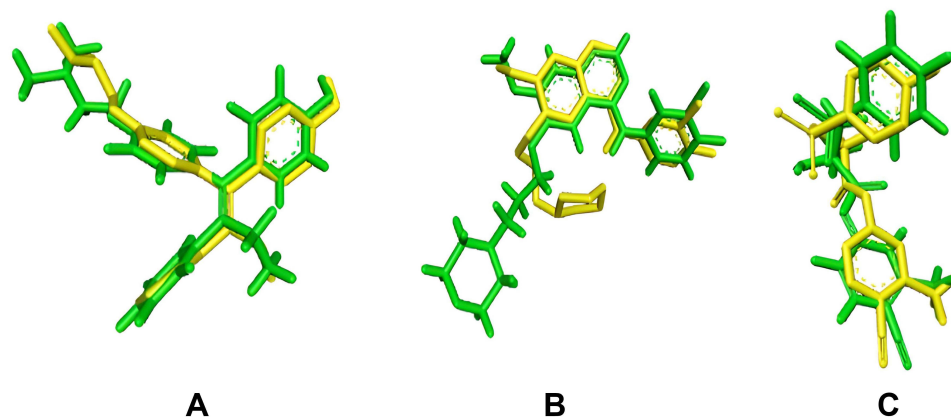

A   **B**   **C**

Figure 6 Overlay results of 3ERT receptor (**A**); 2ITO receptor (**B**); receptor 1Z95 (**C**) (yellow= after *redocking*; green= before *redocking*).

Table 2 Docking Results

Receptor (PDB Code)	Compound	Binding Energy ± SD (kcal/mol)	KI ± SD (nM)
3ERT	Cisplatin	−6.57 ± 0.000	15.23×10^3 ± 0.069
	Bis-(3-methyl-1-(naphthalene-2-carbonyl) thiourea) platinum (II)	−13.21 ± 0.000	0.207 ± 0.215
	Bis-(1-(3-chlorobenzoyl)-3-methyl thiourea) platinum (II)	−9.22 ± 0.000	174.79 ± 0.609
	Bis-(1-(2-chlorobenzoyl)-3-methylthiourea) platinum (II)	−9.21 ± 0.015	177.77 ± 4.349
2ITO	Cisplatin	−6.52 ± 0.000	16.54×10^3 ± 0.032
	Bis-(3-methyl-1-(naphthalene-2-carbonyl) thiourea) platinum (II)	−11.96 ± 0.191	1.77 ± 0.603
	Bis-(1-(3,4-dichlorobenzoyl)-3-methyl thiourea) platinum (II)	−10.69 ± 0.006	14.64 ± 0.089
	Bis-(1-(3-chlorobenzoyl)-3-methyl thiourea) platinum (II)	−10.47 ± 0.000	21.10 ± 0.090
1Z95	Cisplatin	−4.37 ± 0.006	632.21×10^3 ± 6.657
	Bis-(1-(3-chlorobenzoyl)-3-methyl thiourea) platinum (II)	−9.92 ± 0.006	53.85 ± 0.163
	Bis-(1-(2-chlorobenzoyl)-3-methyl thiourea) platinum (II)	−9.86 ± 0.006	58.93 ± 0.413
	Bis-(1-benzoyl-3-methyl thiourea) platinum (II)	−9.00 ± 0.010	253.43 ± 3.644

Drug Scan

The criteria for a good drug must be per *Lipinski's Rule of Five*.[34,35] Drugs given to patients will pass through the body by passing through various pharmacokinetic factors, including absorption, distribution, metabolism and excretion (ADME).[36] *Lipinski's Rule of Five* is commonly used for drugs administered orally; drugs must meet several conditions, including relative molecular weight < 500 g/mol, hydrogen bond donor < 5, Log P < 5, hydrogen bond acceptor < 10, and molar refraction between 40–130.[37] Drug scan results for the platinum (II)-thiourea complexes can be seen in Table 4.

The molecular weight affects the distribution of drugs: the greater the molecular weight, the more difficult for the drug to penetrate the biological membrane, because it has a large molecular size.

Log P is associated with hydrophobicity or lipophilicity, which is the ability of the compound to dissolve in oils, fats, non-polar solvents and lipids. To be absorbed through a lipid bilayer, the drug must have sufficient hydrophobic properties and not be too hydrophobic. If the drug is too hydrophobic, it will be difficult to get out of the bilayer again and cause toxicity because it is in the body longer.

Negative log P values, such as in the case of Bis-(1-benzoyl-3-methyl thiourea)-platinum (II) compounds, are also not recommended; if the drug molecules are too hydrophilic, the drug molecules cannot pass through the lipid bilayer.[38]

The acceptor and donor values of the hydrogen bonds have a relationship with the biological activity of the drug molecule. This biological activity is influenced by the physicochemical properties of compounds, such as the melting point, boiling point, solubility in water, acidity and chelate formation ability.

Molar refraction is the value of the total polarity of a drug molecule and depends largely on the refractive index, temperature and pressure. Polarity is the ease with which molecules form a dipole in a second or sweep a molecule.

The results of the ligand-based drug-likeness (drug scan) screening show that all platinum (II)-thiourea complex compounds meet at least two of the five requirements of the *Lipinski's Rule of Five*, indicating that all complex compounds of platinum (II)-thiourea can be used as an oral preparation.
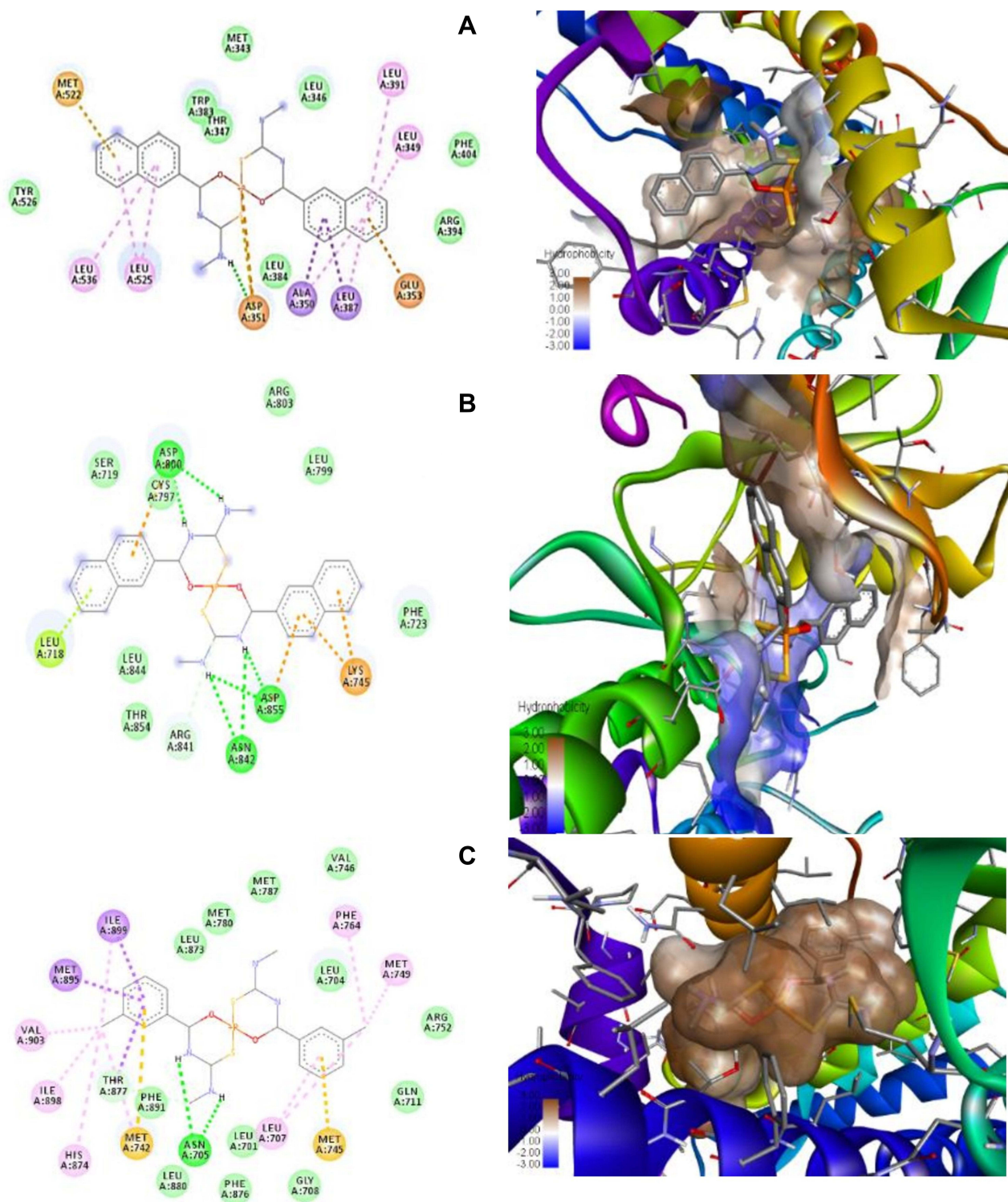
Figure 7 Visualisation of 2D (left) and 3D (right): Bis-(3-methyl-1-(naphthalene-2-carbonyl) thiourea) platinum (II)-3ERT complex (**A**); Bis-(3-methyl-1-(naphthalene-2-carbonyl) thiourea) platinum (II)-2ITO complex (**B**); Bis-(3-methyl-1-(naphthalene-2-carbonyl) thiourea) platinum (II)-1Z95 (**C**).

Pharmacokinetics and Toxicity Predictions

In this study, the prediction of adsorption, distribution, metabolism and toxicity of compounds was carried out using the pKCSM program. The tested compounds consisted of Bis-(1-(3,4-dichlorobenzoyl)-3-methyl thiourea) platinum (II),

Table 3 Interaction Types of Docking Results

PDB Code	Ligand/Compound	Hydrogen Bond	Amino Acid Residues	
			Total	**Amino Acid**
3ERT	Native ligand	3 (ARG A:394; GLU A:353; THR A:347)	22	LEU A:349; GLU A:353; ALA A:350; THR A:347; ARG A:394; LEU A:387; GLY A:521; LEU A:391; HIS A:524; ASP A:351; ILE A:424; MET A:343; LEU A:346; MET A:388; LEU A:525; LEU A:384; MET A:421; PHE A:404; GLY A:420; GLU A:419; LEU A:428; TRP A:383;
	Cisplatin	2 (THR A:347; ASP A:351)	4	ASN A:348; **ALA A:350; ASP A:351; THR A:347;**
	Bis-(3-methyl-1-(naphthalene-2-carbonyl) thiourea) platinum (II)	2 (THR A:347; ASP A:351)	20	**ASP A:351**; VAL A:418; **MET A:343; GLY A:521; THR A:347; MET A:421; GLU A:419**; LEU A:536; TYR A:526; **ALA A:350; GLY A:420; ILE A:424; LEU A:346; LEU A:525**; MET A:522; **LEU A:387; LEU A:384; TRP A: 383; LEU A:349; GLU A:353;**
2ITO	Native ligand	1 (MET A:793)	19	ARG A:841; CYS A:797; GLU A:762; THR A:854; LEU A:788; MET A:766; SER A:719; GLY A:796; ASP A:855; VAL A:726; LEU A:718; ALA A:743; LEU A:844; LYS A:745; THR A:790; MET A:793; PRO A:794; LEU A:792; GLN A:791;
	Cisplatin	2 (ASP A:855; ASN A:842)	6	**CYS A:797; LEU A:844; ARG A:841; THR A:854**; ASN A:842; **ASP A:855;**
	Bis-(3-methyl-1-(naphthalene-2-carbonyl) thiourea) platinum (II)	3 (ASN A:842; ASP A:800; ASP A:855)	13	**SER A:719**; ASP A:800; **CYS A:797**; ARG A:803; LEU A:799; PHE A:723; **LEU A:718; LEU A:844; LYS A:745; ASP A:855; THR A:854; ARG A:841**; ASN A:842;
1Z95	Native ligand	2 (ARG A:752; THR A:877)	24	PRO A:892; PHE A:891; VAL A:903; ILE A:898; HIS A:874; ILE A:899; THR A:877; LEU A:701; ARG A:752; LEU A:704; PHE A:876; LEU A:707; PHE A:764; LEU A:873; MET A:749; ASN A:705; GLN A:711; LEU A:741; MET A:742; MET A:745; MET A:895; GLY A:708; MET A:787; VAL A:746;
	Cisplatin	2 (GLY A:738; HIS A:874)	9	**ILE A:898**; SER A:740; **LEU A:741; MET A:742**; TYR A:739; GLN A:738; **HIS A:874; VAL A:903**; ILE A:906;
	Bis-(1-(3-chlorobenzoyl)-3-methyl thiourea) platinum (II)	1 (ASN A:705)	24	**VAL A:746; ILE A:899; LEU A:873**; MET A:780; **MET A:787; PHE A:764; MET A:749; MET A:895; LEU A:704; ARG A:752; VAL A:903; ILE A:898; THR A:877; GLN A:711; PHE A:891; MET A:742; HIS A:874; ASN A:705**; LEU A:880; **LEU A:707**; LEU A:701; **PHE A:876; MET A:745; GLY A:708;**

Notes: Description: A bolded word indicates an amino acid that is also inert in a native ligand.

Table 4 Drug Scan Results

Compound	Parameters				
	Molecular Weight	Log P	Hydrogen Bond Donor	Hydrogen Bond Acceptor	Refractory Molar
	<500	**<5**	**<5**	**<10**	**40–130**
Bis-(1-(3,4-dichlorobenzoyl)-3-methyl thiourea) platinum (II)	561	6.24	4	6	139.19
Bis-(1-(3-chlorobenzoyl)-3-methyl thiourea) platinum (II)	492	4.93	4	6	129.17
Bis-(1-benzoyl-3-methyl thiourea) platinum (II)	312	−0.05	5	6	777.14

Bis-(1-(3-chlorobenzoyl)-3-methyl thiourea) platinum (II) and Bis-(1-benzoyl-3-methylthiourea) platinum (II). The results of the pKCSM analysis can be seen in Table 5.

The results of the pharmacokinetics and toxicity predictions show that the three platinum (II)-thiourea compounds have good pharmacokinetic parameters, but the Bis-(1-benzoyl-3-methyl thiourea) platinum (II) compounds are mutagenic so cannot be used as the first choice of anticancer agent candidates.

Molecular Dynamics Simulation
Molecular dynamics simulations are carried out to predict the complex interactions of ligand-receptor complexes over time by physical methods of motion and particles. At the time of molecular docking, the proteins used are not in

Table 5 Pharmacokinetics and Toxicity Analysis Results

Parameter	Pharmacokinetic Profile	Bis-(1-(3,4-Dichlorobenzoyl)-3-Methyl Thiourea) Platinum (II)	Bis-(1-(3-Chlorobenzoyl)-3-Methyl Thiourea) Platinum (II)	Bis-(1-Benzoyl-3-Methylthiourea) Platinum (II)
Absorption	CaCO$_2$	0.763	0.768	0.736
	HIA	87.03	91.16	92.83
Distribution	VDss	0.766	0.821	0.826
	BBB	−0.112	−0.054	−0.011
	SSP	−3.621	−2.173	−2.413
Metabolism	CYP 2D6 substrate	No	No	No
	CYP 2D6 inhibition	No	Yes	No
	CYP 3A4 substrate	Yes	Yes	Yes
	CYP 3A4 inhibition	No	Yes	No
	CYP 2C9 inhibition	No	No	No
	CYP 2C19 inhibition	No	No	No
Excretion	Klirens total	−1.026	−1.266	−1.201
Toxicity	Ames test	No	No	Yes
	Hepatoxicities	No	No	No

Notes: Classification: CaCO$_2$ >0.90 = high; HIA <30 = low; VDss ≤0.447 = low, VDss >0.447 = high; BBB >0.3 = well distributed in the brain, BBB <-1 = poorly distributed in the brain; SSP >-2 = distributed both in the SSP, SSP <-3 = difficult to distribute in the SSP.[24]

a flexible state, so the movement of proteins cannot adjust their conformation to ligands. Information about the stability of protein ligands is also known, regardless of space and time, so additional information from simulated molecular dynamics is needed to fill this gap.[39]

The purpose of molecular dynamics simulation is to observe the ligand-receptor interaction over a certain period, according to physiological conditions, to describe the process of action of the drug in the human body.

The ligands selected for molecular dynamics simulation were native ligands, the comparative compound (cisplatin) and the three best test compounds from each of the receptors of breast cancer (3ERT), lung cancer (2ITO) and prostate cancer (1Z95). The three best test compounds of the breast cancer receptor (3ERT) included in the molecular dynamics simulation were Bis-(1-(2-chlorobenzoyl)-3-methyl thiourea) platinum (II), Bis-(1-(3-dichloro benzoyl)-3-methyl thiourea) platinum (II) and Bis-(3-methyl-1-(naphthalene-2-carbonyl) thiourea) platinum (II). The compounds included for the lung receptor (2ITO) were Bis-(1-(3,4-dichlorobenzoyl)-3-methyl thiourea) platinum (II), Bis-(1-(3-chlorobenzoyl)-3-methyl thiourea) platinum (II) and Bis-(3-methyl-1-(naphthalene-2-carbonyl) thiourea) platinum (II), and the compounds included for the prostate cancer receptor (1Z95) were Bis-(1-(2-chlorobenzoyl)-3-methyl thiourea) platinum (II), Bis-(1-(3-chlorobenzoyl)-3-methyl thiourea) platinum (II) and Bis-(1-benzoyl-3-methylthiourea) platinum (II).

Breast Cancer Receptor (3ERT)

The RMSD can be used to observe the stability of interactions between test compounds and breast cancer receptors (3ERT) during the 50 ns simulation (Figure 8). Interactions between breast cancer receptor-ligand complexes (3ERT) showed that the ligand-3ERT complex experienced RMSD fluctuations during 0–3 ns and then had a fairly stable RMSD between 3–50 ns, except for the Bis-(3-methyl-1-(naphthalene-2-carbonyl) thiourea) platinum (II)-3ERT complex, where the RMSD fluctuated again at 35 ns and was then stable until the end of the 50 ns simulation.
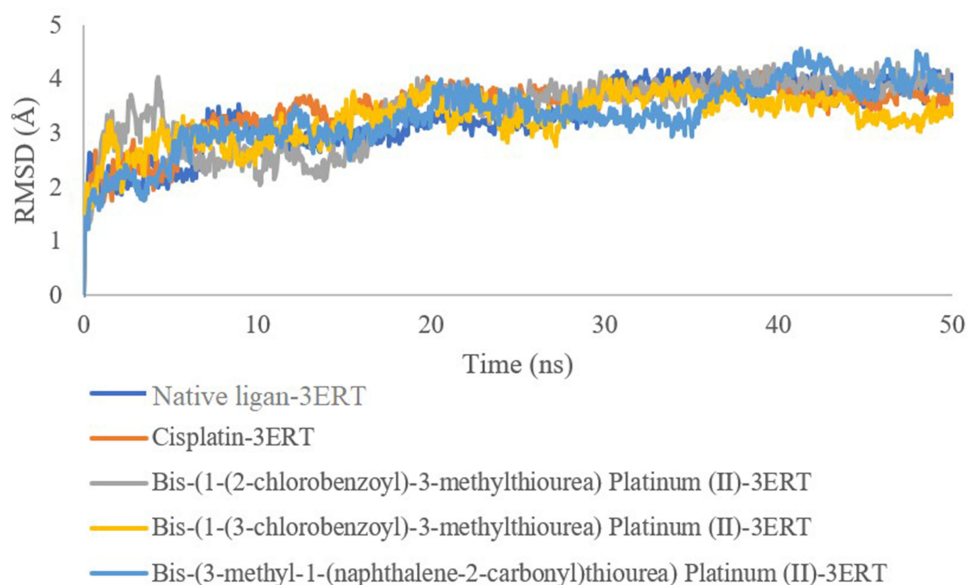
Figure 8 RMSD plot of test compounds – breast cancer receptors (3ERT): natural ligands (light blue), cisplatin (orange), Bis-(1-(2-chlorobenzoyl)-3-methyl thiourea) platinum (II) (grey), Bis-(1-(3-chlorobenzoyl)-3-methyl thiourea platinum (II) (yellow), Bis-(3-methyl-1-(naphthalene-2-carbonyl) thiourea platinum (II) (dark blue).

Thus, it can be concluded that the most stable complex with interaction stability in the simulation of dynamic molecules at 50 ns is the Bis-(1-(3-chlorobenzoyl)-3-methyl thiourea) platinum (II)-3ERT complex, followed by natural ligand-3ERT, Bis-(3-methyl-1-(naphthalene-2-carbonyl) thiourea) platinum (II)-3ERT, Bis-(1-(2-chloroben-zoyl)-3-methyl thiourea) platinum (II)-3ERT and cisplatin-3ERT. This is also supported by the magnitude of the average, minimum and maximum values of RMSD during the 50 ns simulation of each ligand-3ERT complex (Table S4).

The fluctuations in amino acid residues at breast cancer receptors (3ERT) can be seen in the RMSF chart (Figure 9). On the whole, it can be seen that protein-ligand complexes fluctuate in the same region, but the cisplatin (Orange) complex system fluctuates the least. This is reinforced by the average value of each ex-ligand-protein compound: cisplatin-3ERT complex system 1.383 Å, natural ligands-3ERT 1.419 Å, Bis-(1-(2-chlorobenzoyl)-3-methyl thiourea) platinum (II)-3ERT 1.481 Å, Bis-(1-(3-chlorobenzoyl)-3-methyl thiourea) platinum (II)-3ERT 1.454 Å and Bis-(3-methyl-1-(naphthalene-2-carbonyl) thiourea) platinum (II)-3ERT 1.470 Å.

Lung Cancer Receptor (2ITO)

Comparison of the ligand-receptor complexes of lung cancer receptors (2ITO) during the simulation 50 ns (Figure 10) shows that the ligand-2ITO complex experienced RMSD fluctuations from 0–3 ns, then had a fairly stable RMSD between 3–50 ns, except for Bis-(1-(3-chlorobenzoyl)-3-methyl thiourea) platinum (II)-2ITO, where the RMSD fluctu-ated back at 30 ns and was subsequently stable to the end of the 50 ns simulation.

From the RMSD plot in Figure 10, it can be concluded that the most stable complex with interaction stability in the simulation of a dynamic molecule of 50 ns is the Bis-(1-(3,4-dichlorobenzoyl)-3-methyl thiourea) platinum (II)-2ITO complex, followed by natural ligand-2ITO, Bis-(3-methyl-1-(naphthalene-2-carbonyl) thiourea platinum (II)-2ITO, Bis-(1-(3-chlorobenzoyl)-3-methyl thiourea) platinum (II)-2ITO and cisplatin-2ITO. This is supported by the magnitude of the average, minimum and maximum values of RMSD during the 50 ns simulation of each ligand-2ITO complex (Table S5).

The fluctuations in amino acid residues at the lung cancer receptor (2ITO) can be seen in the RMSF chart (Figure 11).

The RMSF plots of the ligand-lung cancer receptor (2ITO) complexes can be used to demonstrate interaction stability, as shown in Figure 11. Overall, it can be seen that the protein-ligand complexes fluctuate in the same region, but the natural ligand complex system-2ITO fluctuates the least. This is reinforced by the average values of each ex-ligand-
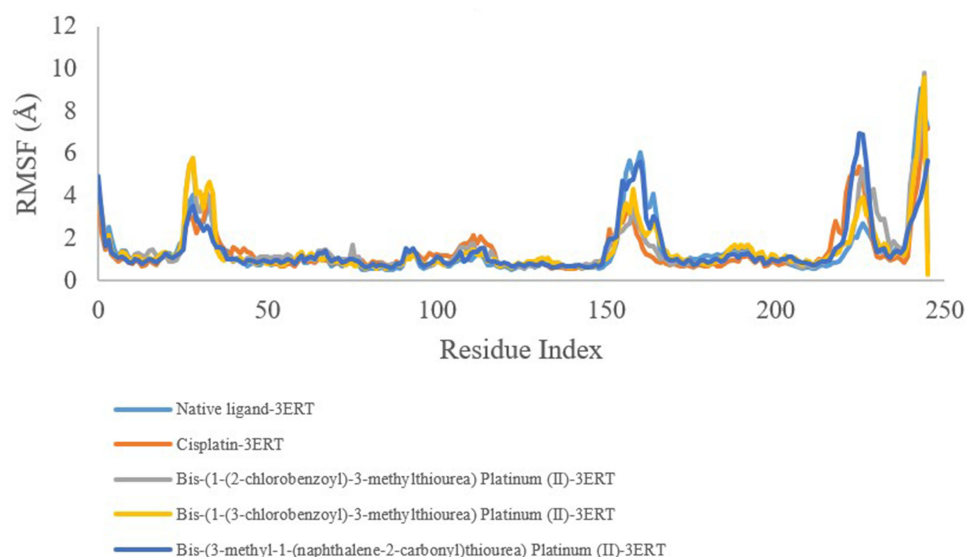
Figure 9 RMSF protein plot of test compounds – breast cancer receptors (3ERT): natural ligands (light blue), cisplatin (orange), Bis-(1-(2-chlorobenzoyl)-3-methyl thiourea) platinum (II) (grey), Bis-(1-(3-chlorobenzoyl)-3-methyl thiourea platinum (II) (yellow), Bis-(3-methyl-1-(naphthalene-2-carbonyl) thiourea platinum (II) (dark blue).
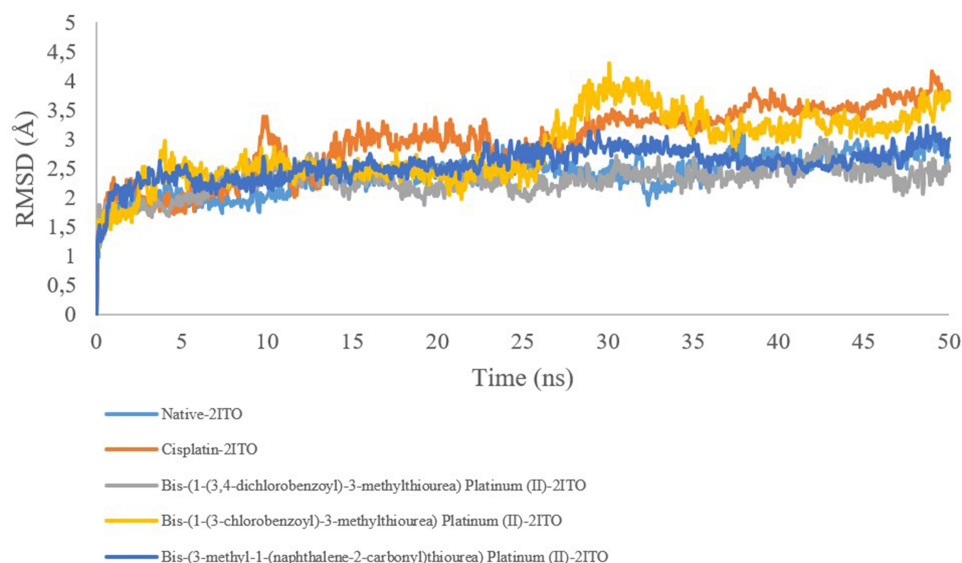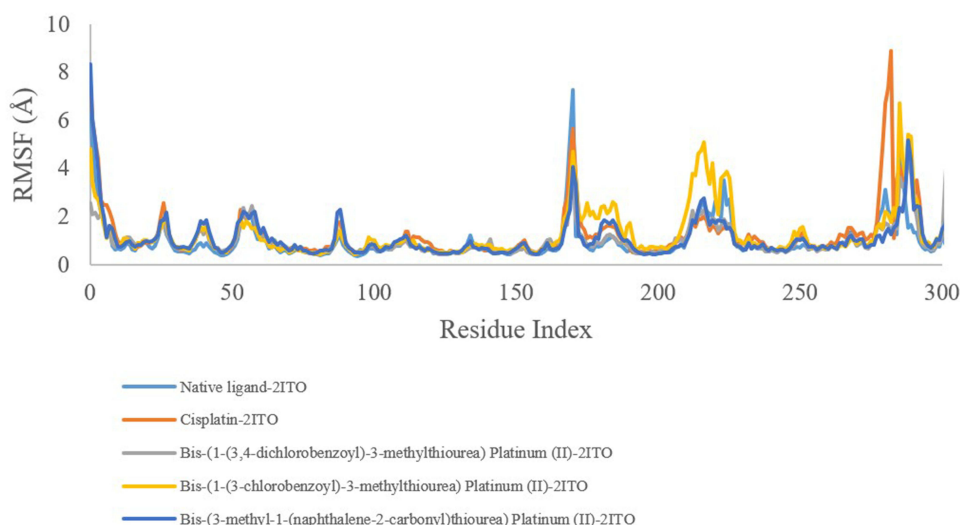

Figure 10 RMSD plot of test compounds – lung cancer receptors (2ITO): natural ligands (light blue), cisplatin (orange), Bis-(1-(3,4-dichlorobenzoyl)-3-methyl thiourea) platinum (II) (grey), Bis-(1-(3-chlorobenzoyl)-3-methyl thiourea platinum (II) (yellow), Bis-(3-methyl-1-(naphthalene-2-carbonyl) thiourea platinum (II) (dark blue).

protein compound: natural ligand complex system-2ITO 1.010 Å, cisplatin-2ITO 1.290 Å, Bis-(1-(3,4-dichlorobenzoyl)-3-methyl thiourea) platinum (II)-2ITO 1.034 Å, Bis-(1-(3-chlorobenzoyl)-3-methyl thiourea) platinum (II)-2ITO 1.296 Å and Bis-(3-methyl-1-(naphthalene-2-carbonyl) thiourea) platinum (II)-2ITO 1.119 Å.

Prostate Cancer Receptors (1Z95)

The interaction between prostate cancer ligand-receptor complexes (1Z95) during 50 ns simulations (Figure 12) shows that the complex interactions of ligands-1Z95, namely natural ligands, Bis-(1-(2-chlorobenzoyl)-3-methyl thiourea) platinum (II), Bis-(1-(3-chlorobenzoyl)-3-methyl thiourea) platinum (II) and Bis-(1-benzoyl-3-methyl

Figure 11 RMSF plot of ligand – lung cancer receptors (2ITO): natural ligands (light blue), cisplatin (orange), Bis-(1-(3,4-dichlorobenzoyl)-3-methyl thiourea) platinum (II) (grey), Bis-(1-(3-chlorobenzoyl)-3-methyl thiourea platinum (II) (yellow), Bis-(3-methyl-1-(naphthalene-2-carbonyl) thiourea platinum (II) (dark blue).
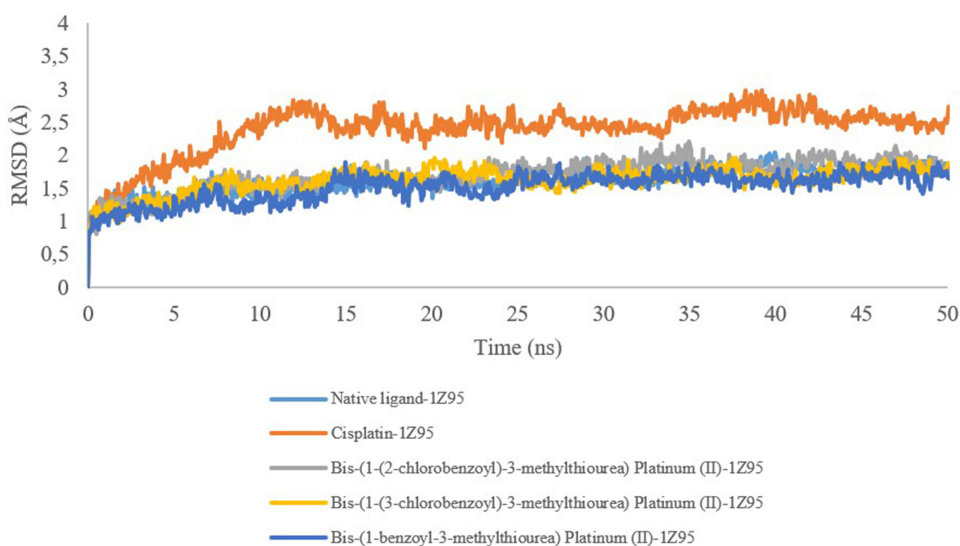
Figure 12 RMSD plot of ligand – prostate cancer receptors (1Z95): natural ligands (light blue), cisplatin (orange), Bis-(1-(2-chlorobenzoyl)-3-methyl thiourea) platinum (II) (grey), Bis-(1-(3-chlorobenzoyl)-3-methyl thiourea) platinum (II) (yellow), Bis-(1-benzoyl-3-methyl thiourea) platinum (II) (dark blue).

thiourea) platinum (II), have RMSDs that fluctuate from 0–7 ns, followed by a fairly stable RMSD from 7–50 ns, until the simulation ends. Meanwhile, the RMSD of the cisplatin comparison compound fluctuates from 0–12 ns, then has a fairly stable RMSD from 12 ns to 50 ns when the simulation ends.

From the RMSD plot in Figure 12, it can be concluded that the complex with the most stable interaction stability in the 50 ns molecular dynamics simulation is the complex Bis-(1-benzoyl-3-methyl thiourea) platinum (II)-1Z95, followed by natural ligand-1Z95, Bis-(1-(3-chlorobenzoyl)-3-methyl thiourea) platinum (II)-1Z95, Bis-(1-(2-chlorobenzoyl)-3-methyl thiourea) platinum (II)-1Z95 and cisplatin-1Z95. This is supported by the magnitude of the average, minimum and maximum values of RMSD during the 50 ns simulation of each ligand-3ERT complex (Table 6).

The fluctuations in amino acid residues at prostate cancer receptors (1Z95) can be seen in the RMSF chart (Figure 13).

Overall, it can be seen in Figure 13 that the protein-ligand complexes fluctuate in the same region, but the natural ligand complex system-1Z95 fluctuates the least. This is reinforced by the average values of each ex-ligand-protein

Table 6 Average, Minimum and Maximum RMSD (1Z95)

Complex System	Average	Minimum	Maximum
Natural Ligand-1Z95	1.609	0.88	2.038
Cisplatin-1Z95	2.387	0.929	2.982
Bis-(1-(2-chlorobenzoyl)-3-methyl thiourea) platinum (II)-1Z95	1.692	0.805	2.209
Bis-(1-(3-chlorobenzoyl)-3-methyl thiourea) platinum (II)-1Z95	1.632	0.765	1.975
Bis-(1-benzoyl-3-methyl thiourea) platinum (II)-1Z95	1.508	0.817	1.904

compound: natural ligand complex system-1Z95 0.749 Å, cisplatin-1Z95 1.033 Å, Bis-(1-(2-chlorobenzoyl)-3-methyl thiourea) platinum (II)-1Z95 0.887 Å, Bis-(1-(3-chlorobenzoyl)-3-methyl thiourea) platinum (II)-1Z95 0.907 Å and Bis-(1-benzoyl-3-methyl thiourea) platinum (II)-1Z95 0.772 Å.

Discussion

The results of the interaction stability evaluation from docking results through MD simulations, looking at RMSD and RMSF graphs, showed that all platinum (II)-thiourea complex compounds selected for the MD 50 ns simulation had a better interaction stability than the comparison compound (cisplatin). Bis-(1-benzoyl-3-methyl thiourea) platinum (II) compounds have the highest interaction stability compared to natural ligands and the comparable compound (cisplatin) when binding to prostate cancer receptors. Bis-(1-(3,4-dichlorobenzoyl)-3-methyl thiourea) platinum (II) compounds have the highest interaction stability compared to natural ligands and the comparative compound (cisplatin) when binding to lung cancer receptors. Bis-(1-(3-chlorobenzoyl)-3-methyl thiourea) platinum (II) compounds have the highest interaction stability compared to natural ligands and the comparable compound (cisplatin) when binding to breast cancer receptors.

The best RMSD complex ligand-protein values for breast cancer (3ERT), lung cancer (2ITO), and prostate cancer (1Z95) receptors are shown in Figure 14A. To observe the flexibility of local residues, the RMSF protein was monitored and the RMSD were evaluated to observe the atomic fluctuations of ligands.[40] One of the RMSF ligands of the Bis-(1-benzoyl-3-methyl thiourea) platinum (II)-1Z95 complex is shown in Figure 14B.

The RMSF plot of the optimal ligand-protein complex for each receptor of breast cancer (3ERT), lung cancer (2ITO) and prostate cancer (1Z95) can be used to demonstrate the stability of the interaction, as shown in
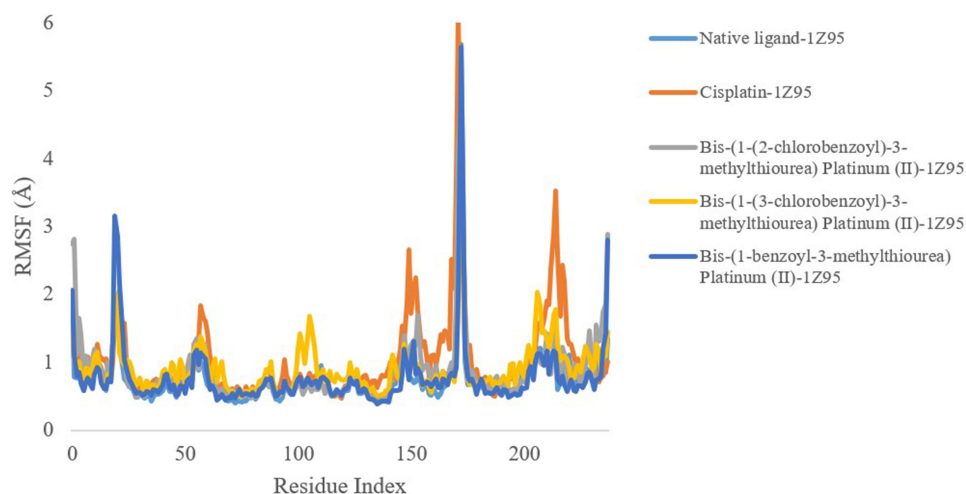

Figure 13 RMSF plot of ligand – prostate cancer receptor (1Z95): natural ligand (light blue), cisplatin (orange), Bis-(1-(2-chlorobenzoyl)-3-methyl thiourea) platinum (II) (grey), Bis-(1-(3-chlorobenzoyl)-3-methyl thiourea) platinum (II) (yellow), Bis-(1-benzoyl-3-methyl thiourea) platinum (II) (dark blue).
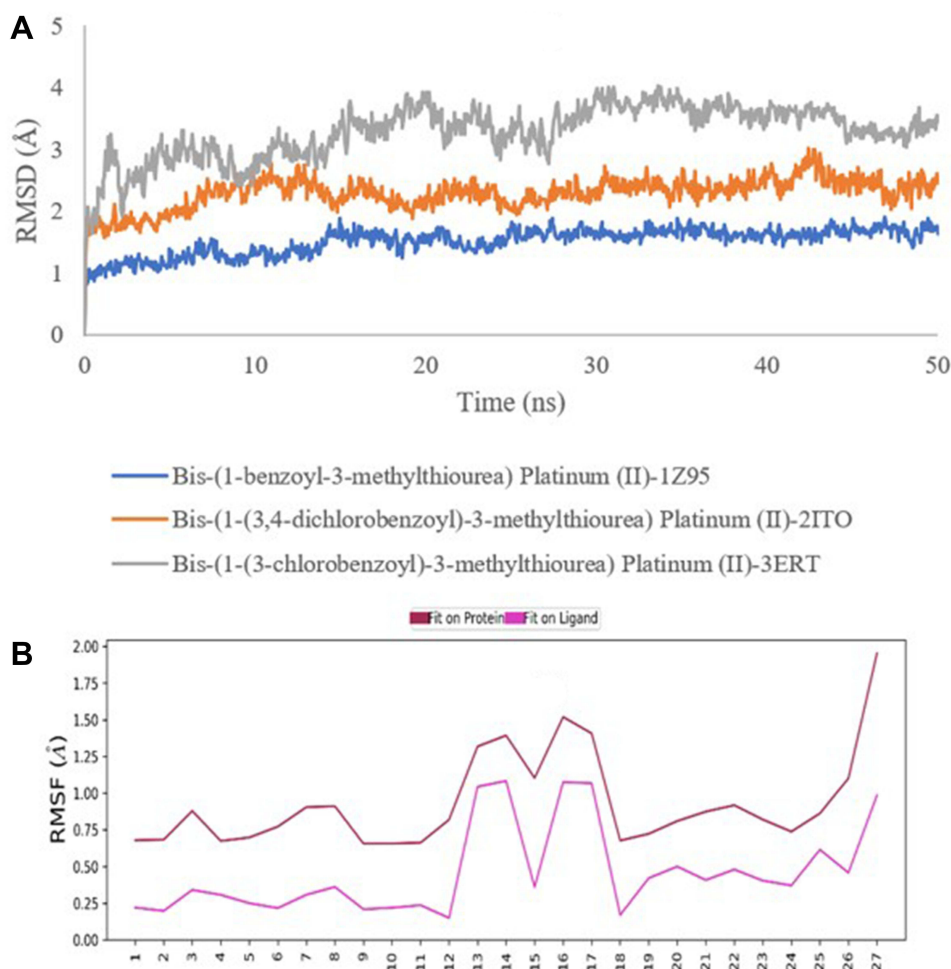
Figure 14 (**A**) RMSD Bis-(1-benzoyl-3-methyl thiourea) platinum (II)-1Z95 (blue), Bis-(1-(3,4-dichlorobenzoyl)-3-methyl thiourea) platinum (II)-2ITO (orange), Bis-(1-(3-chlorobenzoyl)-3-methyl thiourea) platinum (II)-3ERT (grey); (**B**) RMSF ligands from Bis-(1-benzoyl-3-methyl thiourea) platinum (II)-1Z95 compounds.

Figure 13A, where the RMSF chart of the complexes Bis-(1-benzoyl-3-methyl thiourea) platinum (II)-1Z95, Bis-(1-(3,4-dichlorobenzoyl)-3-methyl)thiourea platinum (II)-2ITO and Bis-(1-(3-chlorobenzoyl)-3-methyl thiourea) platinum (II)-3ERT can be seen when simulated at 50 ns. Overall, it can be seen that the protein-ligand complex fluctuates in the same region, but the complex system Bis-(1-benzoyl-3-methyl thiourea) platinum (II)-1Z95 (Blue) fluctuates the least. This is reinforced by the average value of each ligand-protein complex, where the average values of the compounds are as follows: Bis-(1-benzoyl-3-methyl thiourea) platinum (II)-1Z95 0.772 Å, Bis-(1-(3,4-dichlorobenzoyl)-3-methyl thiourea) platinum (II)-2ITO 0.971 Å and Bis-(1-(3-chlorobenzoyl)-3-methyl thiourea) platinum (II)-3ERT 1.355 Å.

Of all the platinum (II)-thiourea complex compounds selected for 50 ns molecular dynamics simulation, the compound Bis-(1-benzoyl-3-methyl thiourea) platinum (II) bound to prostate cancer receptors (1Z95) had the most stable interaction compared to the best platinum (II)-thiourea complex compounds bound to receptors for breast cancer (3ERT) and lung cancer (2ITO).

In addition to being able to see the stability of interactions, RMSF can also be used to see the amino acid residues in contact with the ligands. The RMSF fluctuations of amino acid residues in contact with ligands of the compound Bis-(1-benzoyl-3-methyl thiourea) platinum (II)-1Z95 are shown in Figure 15. The 23 amino acid residues are in contact with compound Bis-(1-benzoyl-3-methyl thiourea) platinum (II)-1Z95 include Leu_701, Leu_704, Asn_705, Leu_707, Gly_708, Leu_712, Leu_741, Met_742, Met_745, Met_749, Phe_764, Met_780, Leu_873, His_874, Thr_877, Leu_880, Phe_891, Pro_892, Met_895, Ile_898, Ile_899 and Val_903, all of which interact through hydrogen bonds, hydrophobic bonds, ions and water bridges, as seen in Figures 16 and 17.
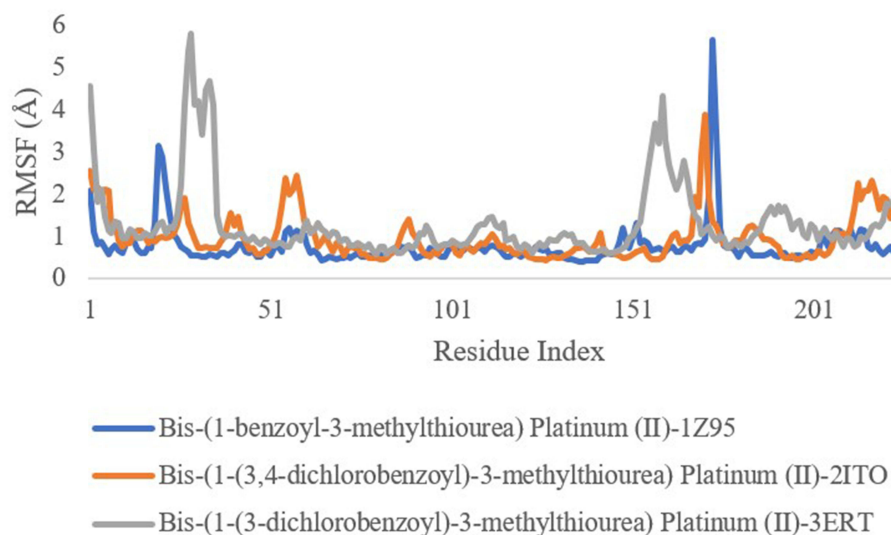
Figure 15 RMSF of Bis-(1-benzoyl-3-methyl thiourea) platinum (II)-1Z95 (blue), Bis-(1-(3,4-dichlorobenzoyl)-3-methyl thiourea) platinum (II)-2ITO (orange), Bis-(1-(3-chlor-obenzoyl)-3-methyl thiourea) platinum (II)-3ERT (grey).
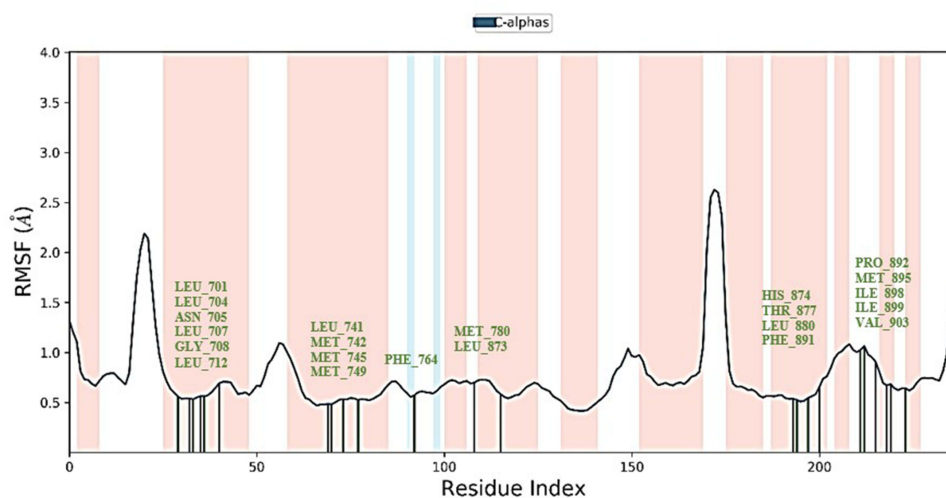

Figure 16 RMSF graph and residual contact on complex systems of Bis-(1-benzoyl-3-methyl thiourea) platinum (II)-1Z95 compounds.
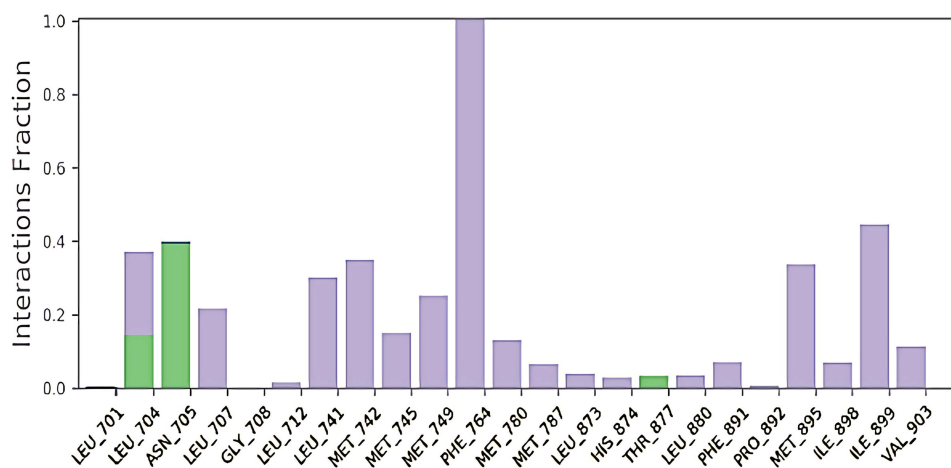

Figure 17 Histogram bar graph showing Bis-(1-benzoyl-3-methyl thiourea) platinum (II)-1Z95 compound in contact residue.

Analysis of the residual contact in the natural ligand complex system-1Z95 shows that there are 23 contact residues (Leu_701, Leu_704, Asn_705, Leu_707, Gln_711, Leu_712, Leu_741, Met_742, Met_745, Val_746, Arg_752, Tyr_763, Phe_764, Met_787, Leu_873, His_874, Phe_876, Thr_877, Leu_880, Met_895, Ile_898, Ile_899, Val_903), while the complex system cisplatin-1Z95 (as a comparison compound) shows 9 contact residues (Gly_708, Ile_737, Gln_738, Tyr_739, Leu_741, Met_742, His_874, Thr_877, Gln_902).

Figure 18 shows that residues interact with ligands in each track frame. Some protein residues show more than one specific contact, with ligands characterised by a darker orange colour. Overall, six parameters were analysed to explain the stability of the Bis-(1-benzoyl-3-methyl thiourea) platinum (II)-1Z95 compound in the 50 ns MD simulation, as shown in Figure 19.

As seen in Figure 19, the RMSD ligand simulation process shows no fluctuations in the initial phase, while fluctuations are observed from 10 to 13 ns, and the RMSD can then be said to be constant from 13 ns to the end of the simulation. No fluctuations were recorded within the gyration radius (rGyr), so the conformation obtained during the 50 ns simulation was stable The SASA plot showed a non-fluctuation pattern during the 50 ns simulation. The MolSA plot showed the bis-(1-benzoyl-3-methyl thiourea) platinum (II)-1Z95 ligand stability during simulation, and the PSA plot was stable until the end of the 50 ns simulation, because it did not experience fluctuations. Meanwhile, the map of intramolecular hydrogen bonds of the Bis-(1-benzoyl-3-methyl thiourea) platinum (II)-1Z95 compound showed no intramolecular hydrogen bonds from the beginning of the simulation to the end of the simulation.

Changes in the interaction of the Bis-(1-benzoyl-3-methyl thiourea) platinum (II)-1Z95 complex can also be seen from the MD simulation results (Figure 20), showing the presence of conformational changes in trajectory during the 50 ns simulation, ranging from 10 ns, 12.5 ns, 25 ns, 37.5 ns and 50 ns. Most of the interacting amino acids from the beginning of the simulation to the end of the dynamic molecular simulation for 50 ns experienced a fairly stable interaction.
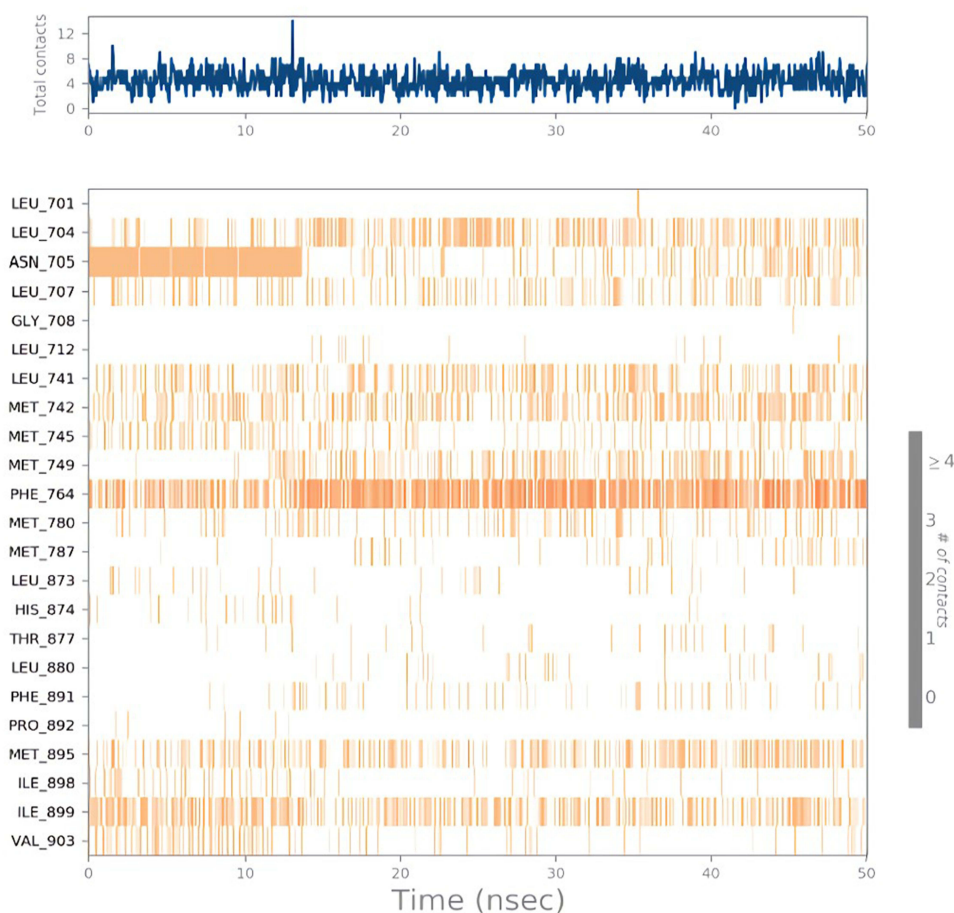

Figure 18 Timeline representation of residual contact in Bis-(1-benzoyl-3-methyl thiourea) platinum (II)-1Z95 in 50 ns MD simulation.
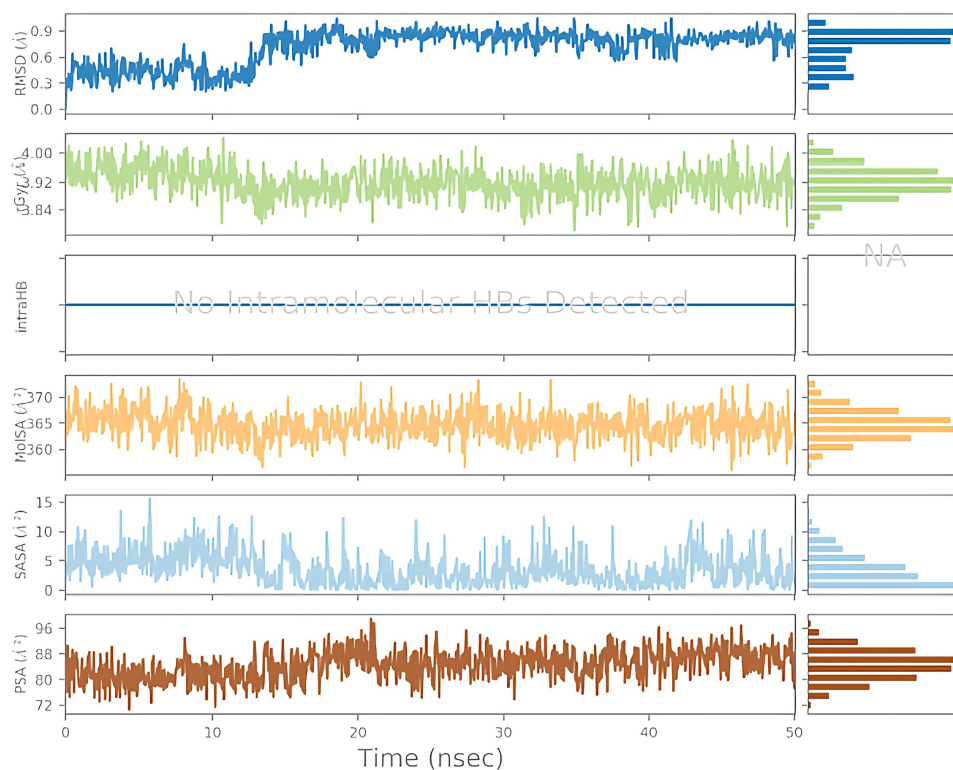
Figure 19 Ligand properties during 50 ns simulation for Bis-(1-benzoyl-3-methyl thiourea) platinum (II)-1Z95 compounds: (**A**) RMSD ligands; (**B**) gyration radius (rGyr); (**C**) intra-hydrogen bond; (**D**) molecular surface area (MolSA); (**E**) solvent accessible surface area (SASA); (**F**) polar surface area (PSA).
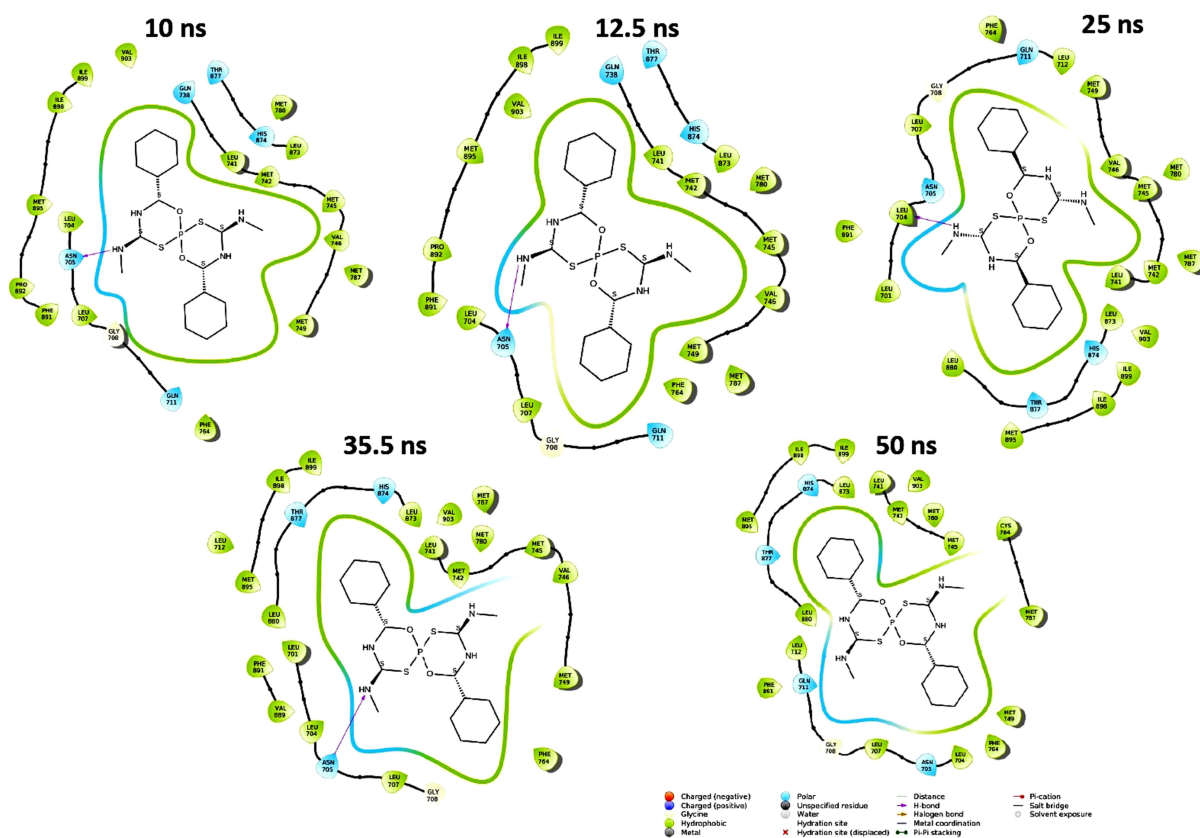

Figure 20 Conformation changes in trajectory of the Bis-(1-benzoyl-3-methyl thiourea) platinum (II)-1Z95 complex in 50 ns MD simulations.

Conclusion

Based on molecular docking, dynamic molecular and pharmacokinetic studies of platinum (II)-thiourea complex compounds that can be used as anticancer agents and do not cause toxicity, Bis-(1-(3,4-dichlorobenzoyl)-3-methyl thiourea) platinum (II) could be a suitable anticancer agent of the lungs.

Acknowledgments

Disclosure

The authors report no conflicts of interest in this work.

References

1. Kerr DJ, Baumann M. *Oxford Textbook of Oncology.* 3rd ed. United Kingdom: Oxford University Press; 2016.
2. Weinberg RA. *The Biology of Cancer.* 2nd ed. New York: Garland Science; 2014.
3. World Health Organization. Cancer. World Health Organization.
4. Hacker M. Adverse drug reactions. In: *Pharmacology.* Academic Press; 2009:327–352.
5. Dilruba S, Kalayda GV. Platinum-based drugs: past, present and future. *Cancer Chemother Pharmacol.* 2016;77(6):1103–1124. doi:10.1007/s00280-016-2976-z
6. Popławska B, Bielawska A, Surażyński A, Czarnomysy R, Bielawski K. Novel dinuclear platinum(II) complexes targets NFkappaB signaling pathway to induce apoptosis and inhibit metabolism of MCF-7 breast cancer cells. *Folia Histochem Cytobiol.* 2009;47(5):S141–146. doi:10.2478/v10042-009-0084-1
7. Czarnomysy R, Bielawska A, Muszyńska A, Bielawski K. Effects of novel alkyl pyridine platinum complexes on apoptosis in Ishikawa endometrial cancer cells. *Med Chem.* 2015;11(6):540–550. doi:10.2174/1573406411666150206163547
8. Bielawski K, Czarnomysy R, Muszyńska A, Bielawska A, Popławska B. Cytotoxicity and induction of apoptosis of human breast cancer cells by novel platinum(II) complexes. *Environ Toxicol Pharmacol.* 2013;35(2):254–264. doi:10.1016/j.etap.2012.12.010
9. Czarnomysy R, Bielawski K, Muszynska A, Bielawska A, Gornowicz A. Biological evaluation of dimethylpyridine–platinum complexes with potent antiproliferative activity. *J Enzyme Inhib Med Chem.* 2016;31(sup3):150–165. doi:10.1080/14756366.2016.1212191
10. Kirishnamaline G, Magdaline JD, Chithambarathanu T, Aruldhas D, Anuf AR. Theoretical investigation of structure, anticancer activity and molecular docking of thiourea derivatives. *J Mol Struct.* 2021;1225. doi:10.1016/j.molstruc.2020.129118
11. Ghorab MM, Alsaid MS, El-Gaby MSA, Elaasser MM, Nissan YM. Antimicrobial and anticancer activity of some novel fluorinated thiourea derivatives carrying sulfonamide moieties: synthesis, biological evaluation and molecular docking. *Chem Cent J.* 2017;11(1):1–14. doi:10.1186/s13065-017-0258-4
12. Miftah AM, Tjahjono DH. Synthesis and in vitro cytotoxicity of 1-benzoyl-3-methyl thiourea derivatives. *Procedia Chem.* 2015;17:157–161. doi:10.1016/j.proche.2015.12.105
13. Fuks L, Anuszewska E, Kruszewska H, Krówczyński A, Dudek J, Sadlej-Sosnowska N. Platinum(II) complexes with thiourea derivatives containing oxygen, sulfur or selenium in a heterocyclic ring: computational studies and cytotoxic properties. *Transit Met Chem.* 2010;35(6):639–647. doi:10.1007/s11243-010-9375-9
14. Ruswanto R. Molecular docking of four isonicotinohydrazide derivatives in mycobacterium tuberculosis enoyl-acyl carrier protein reductase (InhA). *J Kesehat Bakti Tunas Husada.* 2015;13(1):135–141. doi:10.36465/jkbth.v13i1.25
15. Ruswanto R, Nofianti T, Mardianingrum R, Lestari T. Design and in silico study of kuwanon-H derivative compounds as anti-HIV drug candidates. *J Kim Val.* 2018;4(1):57–66. doi:10.15408/jkv.v4i1.6867
16. Victory A, Syahdi RR, Yanuar A. Virtual screening of Indonesian herbal database as murine double minute-2 (MDM2) inhibitor. *Pharmacogn J.* 2018;10(6):1184–1189. doi:10.5530/pj.2018.6.203
17. Puratchikody A, Sriram D, Umamaheswari A, Irfan N. D structural interactions and quantitative structural toxicity studies of tyrosine derivatives intended for safe potent inflammation treatment. *Chem Cent J.* 2016;10:1–19. doi:10.1186/s13065-016-0169-9
18. Ruswanto R, Miftah AM, Tjahjono DH. In silico study of 1-benzoyl-3-methylthiourea derivatives activity as epidermal growth factor receptor (EGFR) tyrosine kinase inhibitor candidates. *Chem Data Collect.* 2021;34:100741. doi:10.1016/j.cdc.2021.100741
19. Tripathi A, Shrinet K, Singh VK, Kumar A. Molecular modelling and docking of mus musculus HMGB1 Inflammatory protein with CGA. *Bioinformation.* 2019;15(7):456–466. doi:10.6026/97320630015456
20. Ruswanto R, Nofianti T, Mardianingrum R, Kesuma D. Design, molecular docking, and molecular dynamics of thiourea-iron (III) metal complexes as NUDT5 inhibitors for breast cancer treatment. *Heliyon.* 2022;8:e10694. doi:10.1016/j.heliyon.2022.e10694
21. Chintha C, Carlesso A, Gorman AM, Samali A, Eriksson LA. Molecular modeling provides a structural basis for PERK inhibitor selectivity towards RIPK1. *RSC Adv.* 2019;10(1):367–375. doi:10.1039/c9ra08047c
22. Blessy JJ, Sharmila DJS. Molecular simulation of N-acetylneuraminic acid analogs and molecular dynamics studies of cholera toxin-neu5gc complex. *J Biomol Struct Dyn.* 2015;33(5):1126–1139. doi:10.1080/07391102.2014.931825
23. Shankar U, Kumar A, Shankar U. Discovery of new hydroxyethylamine analogs against 3CL pro protein target of SARS-CoV-2: molecular docking, molecular dynamics simulation, and structure–activity relationship studies. *J Chem Inf Model.* 2020;60(12):5754–5770. doi:10.1021/acs.jcim.0c00326
24. Pires DEV, Blundell TL, Ascher DB. PkCSM: predicting small-molecule pharmacokinetic and toxicity properties using graph-based signatures. *J Med Chem.* 2015;58(9):4066–4072. doi:10.1021/acs.jmedchem.5b00104

25. Ruswanto R, Garna IM, Tuslinah L, Mardianingrum R, Lestari T, Nofianti T. Quercetin, an inhibitor of uridine 5-monophosphate synthase as an anti-cancer candidate. *ALCHEMY J Penelit Kim*. 2018;14(2):236. doi:10.20961/alchemy.14.2.14396.236-254

26. Gaffar S, Masyhuri AA, Hartati YW, Rustaman R. In silico study of single chain variable fragment (SCFV) Selective for basic natriuretic peptide (BNP) hormone. *Chim Nat Acta*. 2016;4(2):52. doi:10.24198/cna.v4.n2.10671

27. Hasan R, Rony MNH, Ahmed R. In silico characterization and structural modeling of bacterial metalloprotease of family M4. *J Genet Eng Biotechnol*. 2021;19(1). doi:10.1186/s43141-020-00105-y

28. Lemmon G, Meiler J. Towards ligand docking including explicit interface water molecules. *PLoS One*. 2013;8(6):1–12. doi:10.1371/journal.pone.0067536

29. Madhavi Sastry G, Adzhigirey M, Day T, Annabhimoju R, Sherman W. Protein and ligand preparation: parameters, protocols, and influence on virtual screening enrichments. *J Comput Aided Mol Des*. 2013;27(3):221–234. doi:10.1007/s10822-013-9644-8

30. Kolina J, Sumiwi SA, Levita J. Linkage mode of secondary metabolites in yellow root plants (arcangelisia flava L.) with nitric oxide synthase. *FITOFARMAKA J Ilm Farm*. 2019;8(1):45–52. doi:10.33751/jf.v8i1.1171

31. Sari IW, Junaidin J, Pratiwi D. Molecular docking study of the flavonoid compound of orthosiphon stamineus b.) on α-glucosidase receptors as anti-diabetic type 2. *J Farmagazine*. 2020;7(2):54. doi:10.47653/farm.v7i2.194

32. Forli S, Huey R, Pique ME, Sanner MF, Goodsell DS, Olson AJ. Computational protein–ligand docking and virtual drug screening with the AutoDock suite. *Nat Protoc*. 2016;11(5):905–919. doi:10.1038/nprot.2016.051

33. Arwansyah A, Ambarsari L, Sumaryada TI. Docking simulation of curcumin and its analogues as androgen receptor inhibitors in prostate cancer. *Curr Biochem*. 2014;1(1):11–19. doi:10.29244/cb.1.1.11-19

34. Lipinski CA, Lombardo F, Dominy BW, Feeney PJ. Experimental and computational approaches to estimate solubility and permeability in drug discovery and development settings. *Adv Drug Deliv Rev*. 2001;2001:24.

35. Lipinski CA. Lead- and drug-like compounds: the rule-of-five revolution. *Drug Discov Today Technol*. 2004;1(4):337–341. doi:10.1016/j.ddtec.2004.11.007

36. Suhadi A, Rizarullah R, Feriyani F. Docking simulation of the active compound of binahong leaves as an aldose reductase enzyme inhibitor. *Sel J Penelit Kesehat*. 2019;6(2):55–65. doi:10.22435/sel.v6i2.1651

37. Tambunan USF, Amri N, Parikesit AA. Silico design of cyclic peptides as influenza virus, a subtype H1N1 neuraminidase inhibitor. *Afr J Biotechnol*. 2012;11(52):11474–11491. doi:10.5897/ajb11.4094

38. Rachmania RA, Supandi S, Larasati OA. In-silico analysis of the diterpenoid lactone compound of Sambiloto herb (Andrographis Paniculata Nees) on alpha-glucosidase receptors as anti-diabetic type II. *PHARMACY*. 2015;12(2):210–222.

39. Mardiana M. Molecular dynamics simulation of pyridine compounds on 2XNB protein as anticancer using Gromacs applications. *J Min Inst Jpn*. 2019;81(922):235–236.

40. Fatriansyah JF, Rizqillah RK, Yandi MY, Sahlan M, Sahlan M. Molecular docking and dynamics studies on propolis sulabiroin-A as a potential inhibitor of SARS-CoV-2. *J King Saud Univ Sci*. 2022;34(1):101707. doi:10.1016/j.jksus.2021.101707

41. Shiau AK, Barstad D, Loria PM, et al. The structural basis of estrogen receptor/coactivator recognition and the antagonism of this interaction by tamoxifen. *Cell*. 1998;95(7):927–937. doi:10.1016/S0092-8674(00)81717-1

42. Bohl CE, Gao W, Miller DD, Bell CE, Dalton JT. Structural basis for antagonism and resistance of bicalutamide in prostate cancer. *Proc Natl Acad Sci*. 2005;102(17):6201–6206. doi:10.1073/pnas.0500381102

43. Yun C-H, Boggon TJ, Li Y, et al. Structures of Lung Cancer-Derived EGFR Mutants and Inhibitor Complexes: mechanism of Activation and Insights into Differential Inhibitor Sensitivity. *Cancer Cell*. 2007;11(3):217–227. doi:10.1016/j.ccr.2006.12.017